Sorption and mechanism studies of Cu^{2+}, Sr^{2+} and Pb^{2+} ions on mesoporous aluminosilicates/zeolite composite sorbents

Tatyana Kouznetsova, Andrei Ivanets, Vladimir Prozorovich, Ahmad Hosseini-Bandegharaei, Hai Nguyen Tran, Varsha Srivastava and Mika Sillanpää

ABSTRACT

The research aimed to develop a novel mesoporous aluminosilicate/zeolite composite by the template co-precipitation method. The effect of aluminosilicate (AlSi) and zeolite (NaY) on the basic properties and adsorption capacity of the resultant composite was conducted at different mass ratios of AlSi/NaY (i.e., 5/90, 10/80, 15/85, 20/80, and 50/50). The adsorption characteristics of such composite and its feedstock materials (i.e., aluminosilicates and zeolite) towards radioactive Sr^{2+} ions and toxic metals (Cu^{2+} and Pb^{2+} ions) in aqueous solutions were investigated. Results indicated that BET surface area (S_{BET}), total pore volume (V_{Total}), and mesopore volume (V_{Meso}) of prepared materials followed the decreasing order: aluminosilicate (890 m^2/g, 0.680 cm^3/g, and 0.644 cm^3/g) > zeolite (623 m^2/g, 0.352 cm^3/g, and 0.111 cm^3/g) > AlSi/NaY (20/80) composite (370 m^2/g, 0.254 cm^3/g, and 0.154 cm^3/g, respectively). The Langmuir maximum adsorption capacity (Q_m) of metal ions (Sr^{2+}, Cu^{2+}, and Pb^{2+}) in single-component solution was 260 mg/g, 220 mg/g, and 161 mg/g (for zeolite), 153 mg/g, 37.9 mg/g, and 66.5 mg/g (for aluminosilicate), and 186 mg/g, 140 mg/g, and 77.8 mg/g for (AlSi/NaY (20/80) composite), respectively. Ion exchange was regarded as a domain adsorption mechanism of metal ions in solution by zeolite; meanwhile, inner-surface complexation was domain one for aluminosilicate. Ion exchange and inner-surface complexation might be mainly responsible for adsorbing metal ions onto the AlSi/NaY composite. Pore-filling mechanism was a less important contributor during the adsorption process. The results of competitive adsorption under binary-components (Cu^{2+} and Sr^{2+}) and ternary-components (Cu^{2+}, Pb^{2+}, and Sr^{2}) demonstrated that the removal efficacy of target metals by the aluminosilicate, zeolite, and their composite remarkably decreased. The synthesized AlSi/NaY composite might serve as a promising adsorbent for real water treatment.

Key words | adsorption, heavy metal, mesoporous aluminosilicate, radioactive ion, textural property, zeolite

HIGHLIGHTS

- A simple and green route of composite sorbents preparation was developed.
- The sorption properties of prepared composites towards Cu^{2+}, Sr^{2+}, and Pb^{2+} ions were studied in single and multicomponent model solution.
- The sorption mechanism was proposed.

Tatyana Kouznetsova
Andrei Ivanets (corresponding author)
Vladimir Prozorovich
Institute of General and Inorganic Chemistry of National Academy of Sciences of Belarus,
St. Surganova 9/1, 220072 Minsk,
Belarus
E-mail: *ivanets@igic.bas-net.by*

Ahmad Hosseini-Bandegharaei
Department of Environmental Health Engineering, School of Health,
Sabzevar University of Medical Sciences,
Sabzevar,
Iran
and
Department of Engineering, Kashmar Branch,
Islamic Azad University, P.O. Box
161, Kashmar,
Iran

Hai Nguyen Tran
Institute of Fundamental and Applied Sciences,
Duy Tan University,
Ho Chi Minh 700000,
Vietnam

Hai Nguyen Tran
Mika Sillanpää
Faculty of Environmental and Chemical Engineering,
Duy Tan University,
Da Nang 550000,
Vietnam

Varsha Srivastava
Department of Chemistry,
University of Jyväskylä,
P.O. Box 35, FI-40014, Jyväskylä,
Finland

Mika Sillanpää
Institute of Research and Development,
Duy Tan University,
Da Nang 550000,
Vietnam
and
School of Civil Engineering and Surveying, Faculty of Health, Engineering and Sciences,
University of Southern Queensland,
West Street, Toowoomba, 4350 QLD,
Australia

doi: 10.2166/wst.2020.407

INTRODUCTION

Aluminosilicates are widely used as catalysts (Yang *et al.* 2007; Lopes *et al.* 2014; Li *et al.* 2016) and adsorbents of heavy metals, dyes, and other toxic contaminants (Tsai *et al.* 2019; Liang *et al.* 2020). Currently, many researchers are trying to find more appropriate ways for the removal of heavy metals from aqueous media, because of their high toxicity and their ability to accumulate in living organisms (Chowdhury *et al.* 2018). In this context, aluminosilicates are potential materials for the efficient sorption of metal ions from solutions at the solid/liquid interface. According to WHO recommendations, the maximum permissible concentrations in water for different metals such as Cu^{2+} (2.0 mg/L) and Pb^{2+} (0.01 mg/L) (WHO 2011). There is not a federal drinking water standard for Sr^{2+} at this time. However, for example, the US Environmental Protection Agency (EPA) has set a health reference level for strontium. The health reference level for strontium in water was listed as 4.0 mg/L (Patil *et al.* 2016).

Adsorption processes successfully compete with the methods of coagulation (Chowdhury *et al.* 2018), reverse osmosis (Jamaly *et al.* 2014), chemical deposition (Tao *et al.* 2014), electrolysis (Wang *et al.* 2020), and ion exchange (Sepehrian *et al.* 2010) in drinking water treatment for achieving these permissible values. Currently, natural and synthetic zeolites are widely studied as adsorbents of various inorganic (i.e., potentially toxic metals) (Chao & Chen 2012) and organic (4-nitrophenol) (Kalaycı & Bardakçı 2014) contaminants. When using zeolite adsorbents for sorption purposes, major objectives are to increase the sorption capacity and selectivity (Zayed *et al.* 2017). Typically, this is achieved by varying the synthesis conditions and the choice of different modifiers for the amelioration of the porous structure and chemical nature of the surface.

Zayed *et al.* (2017) described the synthesis of NaA zeolites by preparing zeolite by calcination (ZC) and zeolite by alkali fusion (ZF) from Egyptian kaolinite. The influence of initial Mn^{2+} concentration, contact time, and zeolite dose on the Mn^{2+} adsorption performance of the obtained zeolites was studied. The adsorption characteristics for Mn^{2+} were well described using the Langmuir isotherm model and the pseudo-second-order kinetic relation. Qian & Li (2015) prepared NaA zeolite (NAZ) using coal gangue (CG) as the raw material via the *in-situ* crystallization technique. Firstly, CG was decarbonized at 800 °C to form an X-ray amorphous material. Secondly, the hydrothermal treatment was performed in aqueous alkali to form the NAZ crystal. The synthetic NAZ exhibited excellent calcium binding capacity compared to the commercial-grade NAZ. Equilibrium and kinetic studies for the adsorption of iron from aqueous solution by the synthetic NaA zeolites were carried out by Seliem & Komarneni (2016). The behavior of iron uptake by each synthetic zeolite was evaluated by studying the influence of different experimental parameters such as contact time, initial iron concentration, and the dried zeolite's mass.

For enhancing sorption properties, Wang *et al.* (2017) synthesized single- or dual-cation organomontmorillonites (OMt) modified by one or two cationic surfactants, respectively, and/or cysteamine hydrochloride (CSH). The adsorption results of Zn^{2+} showed that OMt had much higher adsorption capacities than Na^{+}-Mt. The process of Zn^{2+} adsorption onto dual-cation OMt was due to ion exchange, the formation of complexes, and/or precipitation mechanism (depending on the solution pH values). A series of reduced-charge montmorillonites (RCMs) were modified by hexamethylene bispyridinium dibromides (HMBP) and then used to remove phenols from aqueous solution. The effects of concentration of HMBP, clay layer charge, contact time, temperature, and pH were investigated using a batch technique. The results implied that the clay layer charge had a significant influence on phenol adsorption (Luo *et al.* 2015a). Organoclays were obtained by modifying a series of reduced charge montmorillonites (RCMs) using three Gemini surfactants with different spacer lengths, and their structures and adsorption characteristics for methyl orange (MO) were examined. The results suggested that the amount, spacer length of Gemini surfactant, and clay layer charge had significant effects on the microstructure of the organoclays (Luo *et al.* 2015b).

In this work, a new adsorbent (composite) was developed by the combination of the excellent ion-exchange properties of zeolite and the advantages of mesoporous ordered aluminosilicate. The adsorption efficiency of three metal ions (Cu^{2+}, Sr^{2+}, and Pb^{2+}) onto such a new composite was compared with that of its feedstock parent (i.e., zeolite and aluminosilicate). The novelty statement of this manuscript includes that (1) a simple and green route of composite's preparation was developed, (2) the adsorption properties of the prepared composite towards Cu^{2+}, Sr^{2+}, and Pb^{2+} ions were studied in single- and multi-component solution, and (3) the adsorption mechanism is discussed herein.

MATERIALS AND METHODS

Preparation of adsorbent

The ordered mesoporous aluminosilicate with various Al_2O_3/SiO_2 weight ratios (%) was synthesized by hydroxide coprecipitations under the presence of supramolecular template by neutralization of aluminum sulfate and liquid glass solutions. Cetylpyridinium chloride (5.0% concentration) was added into a previously heated (at 40 °C) aqueous solution of liquid glass (13729 Sigma-Aldrich; $NaOH \geq 10\%$; $SiO_2 \geq 27\%$; and density of 1.39 g cm^{-3} at 20 °C) with the SiO_2 content of 5.5 wt.%. For the neutralization of NaOH, sulfuric acid (35 wt.%) was introduced into the solution and the mixture was then kept for 30 min at 40 °C. The concentrated aqueous solution of aluminum sulfate was added to the reaction mixture. After mixture aging for 10 min at 40 °C, the pH value was adjusted to 6.0 by a dilute solution of ammonia hydrate (1:1).

Commercial NaY zeolite (well-dispersed in water) with a typical oxide formula ($Na_2O \times Al_2O_3 \times 4.8SiO_2 \times H_2O$) was added to the reaction mixture. The weight ratios of mesoporous ordered aluminosilicate and NaY zeolite were 50/50, 20/80, 15/85, 10/90, and 5/95 (wt%/wt%). Subsequently, the precipitates were separated and dried at room temperature. For increasing cation exchange capacity, the resultant xerogel was respectively suspended in a 3.0 wt.% ammonium sulfate aqueous solution, twice in a solution with pH 9.0 and in a solution of ammonia hydrate (1:1). After that, the xerogel was twice washed with distilled water and heated at 60 °C. After the filtered xerogel had been dried in the air and then in a desiccator at 120 °C, it was heated at 650 °C for 2 h to obtain the resultant aluminosilicate/zeolite composite. The Na_2O content in the pristine aluminosilicate was around 0.1 wt.%.

Nitrogen adsorption-desorption isotherm

The textural properties of the prepared solid samples were calculated from the isotherms of physical adsorption/desorption of nitrogen at a fixed low temperature (77 K) that was measured by an analyser of surface area and porosity (ASAP 2020 MP). The surface area of the pores per unit mass of solids was calculated from the Brunauer–Emmett–Teller (BET) equation (S_{BET}). The other parameters – surface areas of micropores (S_{Micro}) and external surface (S_{Ext})–were determined using the comparative *t*-plot method, considering $S_{Micro} = S_{BET} - S_{Ext}$ and $S_{BET} > S_{Ext}$. The calcined samples had been vacuumed (residual pressure of 133.3×10^{-3} Pa) at the temperature of 523 K for 2 hours before they were analysed by the textual properties. The relative error of the pore volume was ±1%; meanwhile that of surface area and pore size was ±15%.

Scanning electron microscopy (SEM) and energy dispersive X-ray spectroscopy (EDX)

The surface morphology of the mesoporous aluminosilicate/zeolite composite and their feedstocks was explored by a scanning electron microscope (JSM-5610 LV). The main elemental composition on their surface was evaluated with the system of point chemical analysis EDX JED-2201 JEOL (Japan).

Adsorption study of metal ions

To study the influence of initial concentration of Cu^{2+}, Sr^{2+}, and Pb^{2+} ions on the adsorption capacity of the prepared adsorbents, the single-component solutions were used by different metal concentrations in a range from 50 to 1,000 mg/L. Approximately 0.04 g of each adsorbent was mixed with 10 mL of model solution ($pH = 5.0 \pm 0.2$) at room temperature (~30 °C) for a fixed contact time of 24 h. The equilibrium concentration of the cations in the solution was determined by atomic absorption analysis on the ContrAA300 spectrometer (Analytic Jena, Germany).

Adsorption from a bi-component (Cu^{2+} and Sr^{2+}) and multi-component (Cu^{2+}, Sr^{2+}, and Pb^{2+}) solution was carried out under similar experimental conditions such as the concentration of each metal cation of 200 mg/L, weight of adsorbents 0.04 g, and 10 mL of target solution ($pH = 5.0 \pm 0.2$).

The obtained data were used for modelling experimental adsorption isotherms. They were fitted to the Langmuir and Freundlich isotherm models (Equations (1) and (2), respectively) which are most often used for the description of the adsorption process of solid-liquid phase. The equations of isotherm models exploited in this research are given in Equations (1) and (2) (Tran *et al.* 2017b).

$$q_e = \frac{Q_m K_L C_e}{1 + K_L C_e} \quad (1)$$

$$q_e = K_F C_e^{1/n_F} \quad (2)$$

where q_e is the adsorption capacity (mg/g) of adsorbate by adsorbent at an equilibrium time; C_e is the equilibrium concentration of adsorbate (mg/L); Q_m and K_L are the maximum adsorption capacity of adsorbent (mg/g) and the Langmuir constant (L/mg), respectively; and K_F [(mg/g)/(L/mg)^{nF}] and n_F are the Freundlich adsorption constants.

RESULTS AND DISCUSSION

Textural property of the aluminosilicate, zeolite, and AlSi/NaY composites

According to the IUPAC classification (Thommes *et al.* 2015), the adsorption/desorption isotherm of nitrogen at 77 K (Figure 1(a)) are categorized as Type IV for aluminosilicate (AlSi), with a hysteresis loop being Type H4 (Sepehrian *et al.* 2010; Tsai *et al.* 2019).The result suggested that AlSi is a typical mesoporous material (Table 1). In contrast, zeolite (NaY) exhibits the Type I isotherm of nitrogen physisorption and the Type H4 hysteresis loop that are typical characteristics of a dominantly microporous material (high S_{Micro}) (Morales-Ospino *et al.* 2020) with its relatively-low external surface area (low S_{Ext}). Meanwhile, the nitrogen physisorption isotherms of the new AlSi/NaY composites (Figure 1(b)) are relatively close to Type IV. However, their hysteresis loops (Type H4 or H3) are strongly dependent on the ratio of AlSi and NaY used (Thommes *et al.* 2015).

The calculated results from the isotherms of nitrogen adsorption/desorption are provided in Table 1. The aluminosilicate (890 m^2/g and 0.680 cm^3/g) exhibited a larger S_{BET} and higher V_{Total} values than the zeolite (623 m^2/g and

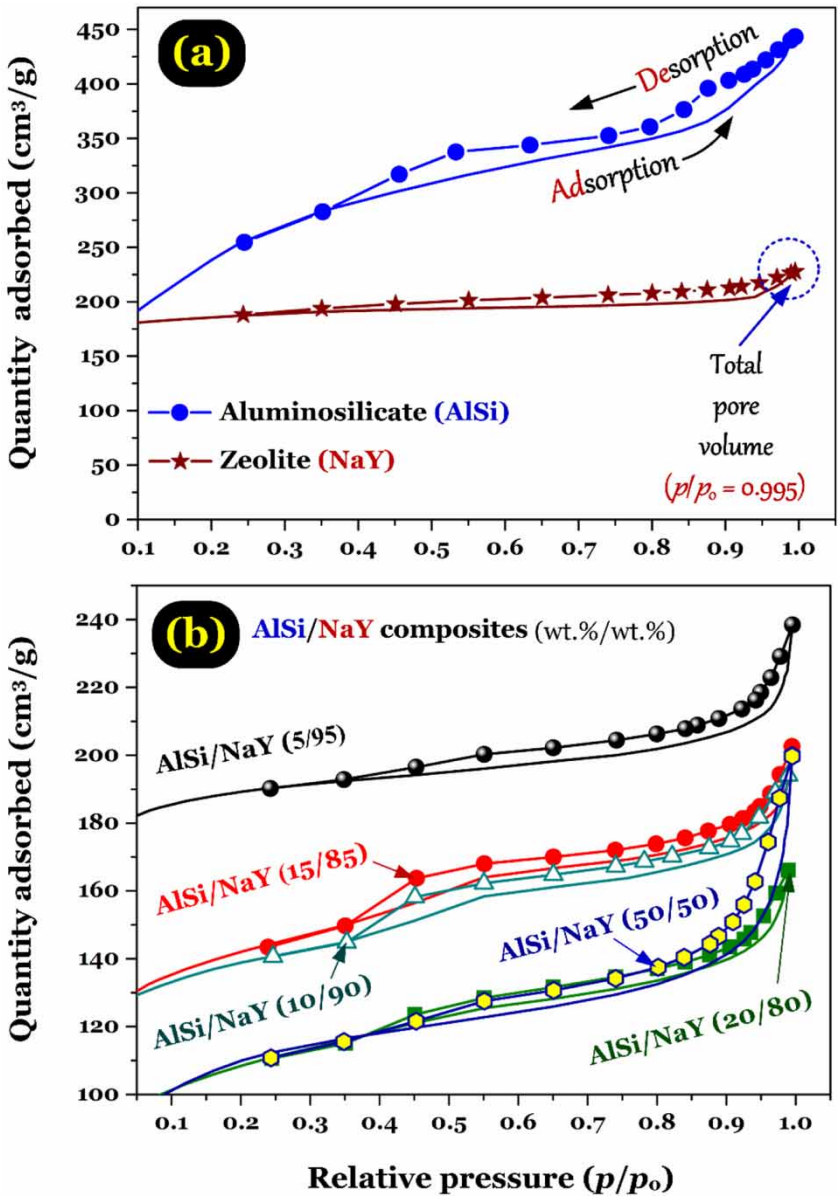

Figure 1 | Nitrogen adsorption/desorption isotherm at 77 K of (a) pristine aluminosilicate and pristine zeolite and (b) their composites.

Table 1 | Textural parameters of pristine mesoporous aluminosilicate (AlSi), pristine zeolite (NaY), and their composites (AlSi/NaY; wt.%/wt.%)

	Surface area (m^2/g)				Pore volume (cm^3/g)				
	S_{BET}	S_{Lang}	S_{Ext}	S_{Micro}	V_{Total}	V_{Micro}	V_{Meso}	V_{Meso} (%)	Average pore width (nm)
Aluminosilicate (AlSi)	**890**	1,258	705	185	**0.680**	0.037	0.644	**94.6**	3.06
Zeolite (NaY)	**623**	823	105	518	**0.352**	0.241	0.111	**31.5**	2.26
AlSi/NaY (5/95)	631	837	81	550	0.347	0.257	0.090	26.0	2.20
AlSi/NaY (10/90)	469	623	123	347	0.297	0.161	0.136	45.7	2.53
AlSi/NaY (15/85)	480	642	147	333	0.295	0.155	0.140	47.4	2.46
AlSi/NaY (20/80)	**370**	498	155	216	**0.254**	0.100	0.154	60.6	2.74
AlSi/NaY (50/50)	**380**	509	184	196	**0.277**	0.089	0.188	67.9	2.91

0.252 cm^3/g) did, respectively. For the AlSi/NaY composites, an increase in the amount of AlSi used (wt.%) led to remarkably decreasing textural parameters (i.e., S_{BET} and V_{Total}) of the resultant composites (Table 1). The decreases might result from the zeolitization phenomenon (Wang *et al.* 2002). The change of textual properties of the AlSi/NaY composites compared to their feedstocks (AlSi and NaY) might result in changing their adsorption capacity and behavior towards toxic metals in water solution.

Surface morphology and element component properties of the aluminosilicate, zeolite, and AlSi/NaY composites

The distinctions in the external morphologies (interior features) of zeolite, aluminosilicate, and their composites are well visible in Figure 2. Zeolite is created from the interparticle agglomerates, with the size ranging approximately from 5 μm to10 μm. The aggregated crystals of zeolite (Figure 2(a)) created the dominantly-microporous property of NaY (Table 1). A similar surface morphology was observed in the composite, with the ratio of AlSi to NaY being 5–95 (Figure 2(c)). In contrast, the mesoporous aluminosilicate exhibited agglomerates (50–200 μm size) significantly larger than the zeolite and had a high-ordered supramolecular structure (Figure 2(b)). This structure might be partly maintained in the AS/NaY composite because of the features of adhesion in the system of two solid bodies – aluminosilicate and NaY zeolite.

The chemical elements (present on the surface of NaY zeolite, aluminosilicate, and their composite) were analysed by the EDX method, and the results are provided in Figure 2(d)–2(f). Clearly, EDX spectra confirmed the similarity of the chemical nature between aluminosilicate and zeolite. Therefore, the contacting components are charged the same (negatively) and therefore there is no counter diffusion. In the EDX spectrum of zeolite (Figure 2(d)), the energy peaks at 0.525, 1.041, 1.486, and 1.739 keV are related to the O, Na, Al, and Si elements, respectively. The main peaks of O, Na, Al, and Si were also shown in the EDX spectrum of the AlSi/NaY composite (Figure 2(f)). The results confirmed that the chemical composition and structure of zeolite might not significantly change during the formation of the AlSi/NaY composite. In the EDX spectrum of aluminosilicate (Figure 2(e)), peak in the region of 1.041 keV (related to the Na atoms) was absent. Notably, the content of Na atoms was observed at 10.04 and 5.02 at.% for the NaY zeolite and AlSi/NaY composite, respectively. This is confirmed by the lack of sodium in aluminosilicate.

The main functional groups on the surface of the AlSi/NaY (20/80) composite are provided in Figure 3. Because the aluminosilicate and zeolite materials possessed similar components on its surface (main C, O, Si, and Al atoms), it is not easy to distinguish the surface functionalities on their composite. For example, an intense band at around 1005 cm^{-1} is the overlap of the Si–O–Si group on the surface of aluminosilicate (Nampi *et al.* 2010; Sepehrian *et al.* 2010) and the O–T–O group on the surface of zeolite (T denoting Si or Al) (Kalaycı & Bardakçı 2014; Huang *et al.* 2016). Similarly, the presence of hydroxyl group (–OH) is well-identified at approximately 3,500 cm^{-1} that is the overlap of the –OH groups on the surfaces of aluminosilicate and zeolite (Sepehrian *et al.* 2010; Huang *et al.* 2016). Some other bands were observed in the Fourier transform infrared (FTIR) spectrum at around 463 and 570 cm^{-1} (T–O in zeolite) (Kalaycı & Bardakçı 2014; Huang *et al.* 2016), 693 and 770 cm^{-1} (Si–O–Al in aluminosilicate) (Nampi *et al.* 2010; Tsai *et al.* 2019), and 1,646 cm^{-1} [$\delta_{OH}(H_2O)$] (Sepehrian *et al.* 2010). The results demonstrated that the AlSi/NaY (20/80) composite exhibited abundant oxygen-functional groups on its surface. Such groups have been reported to

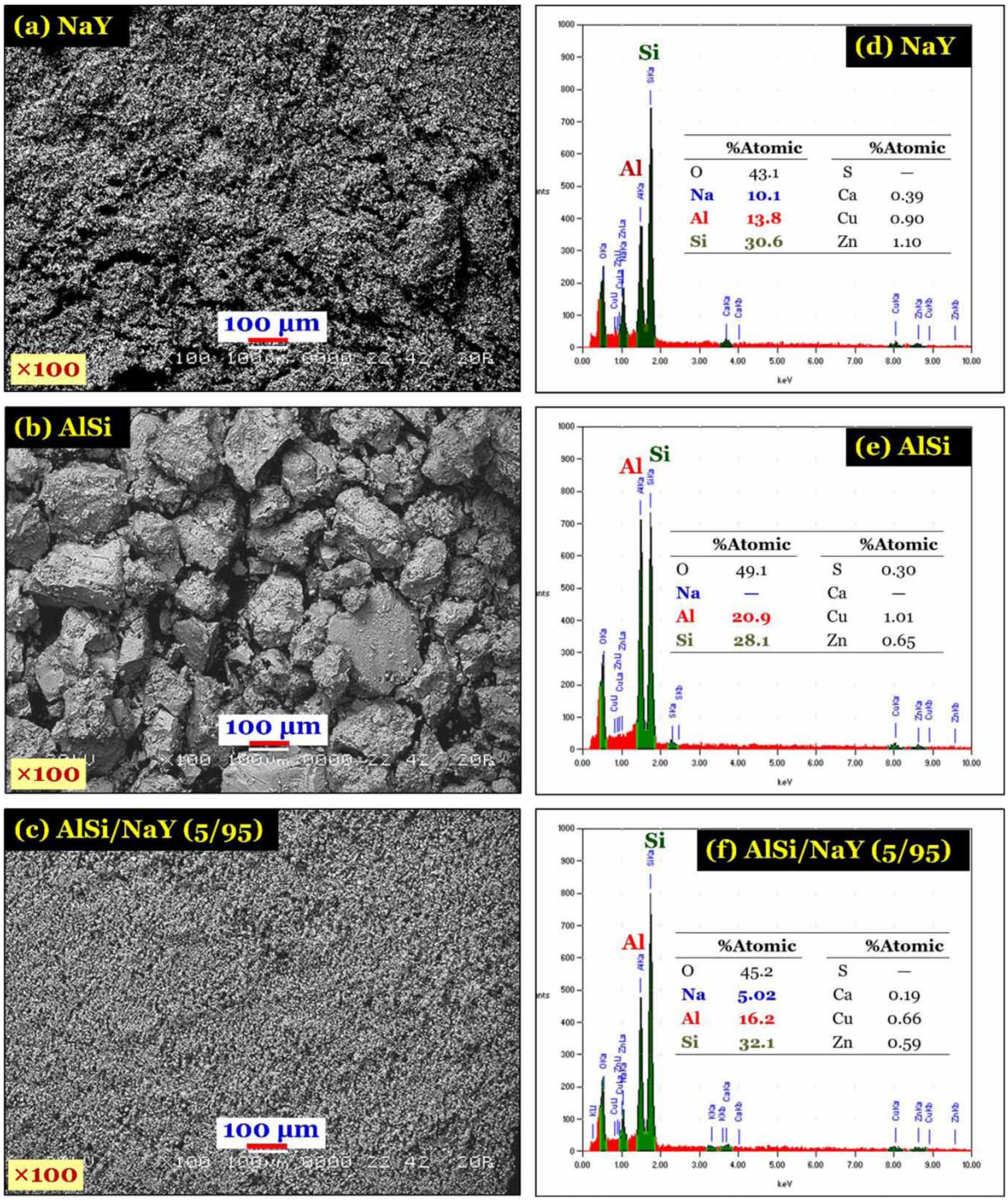

Figure 2 | (a)–(c) SEM image and (d)–(f) EDX spectrum of NaY, AlSi and their AlSi/NaY composite.

effectively bind metal ions in solution through surface complexation (Tran *et al.* 2019; Tsai *et al.* 2019; Liang *et al.* 2020).

The crystal structure of the AlSi/NaY (20/80) composite is indicated in Figure 4. In essence, the aluminosilicate and zeolite solids shared similar X-ray diffraction (XRD) patterns (Nampi *et al.* 2010; Watanabe *et al.* 2010; Qian & Li 2015; Zayed *et al.* 2017; Liang *et al.* 2020). Therefore, the peak locations indicating the crystals of zeolite and aluminosilicate nearly overlapped (Figure 4).

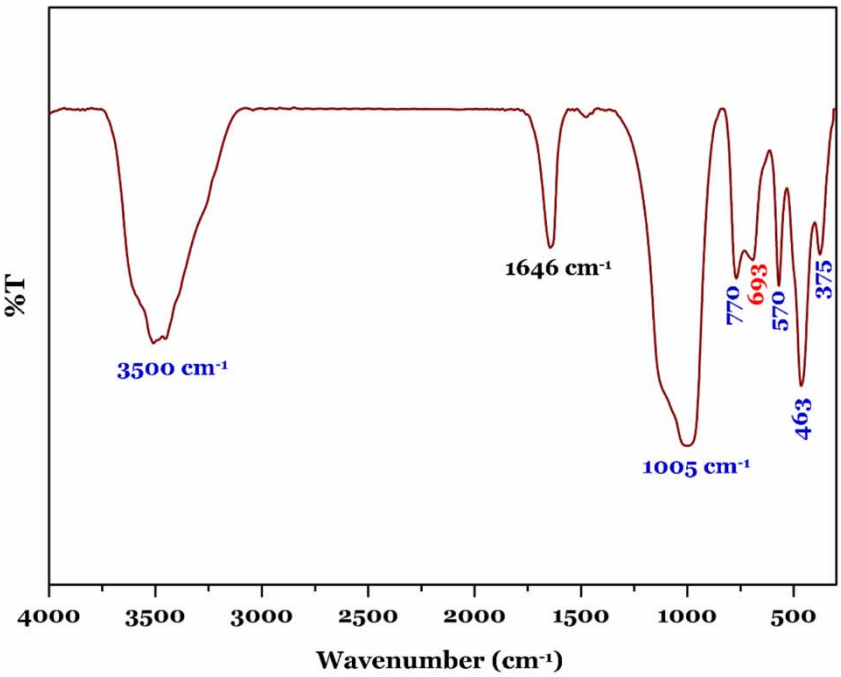

Figure 3 | FTIR spectrum of the composites AlSi/NaY (20/80).

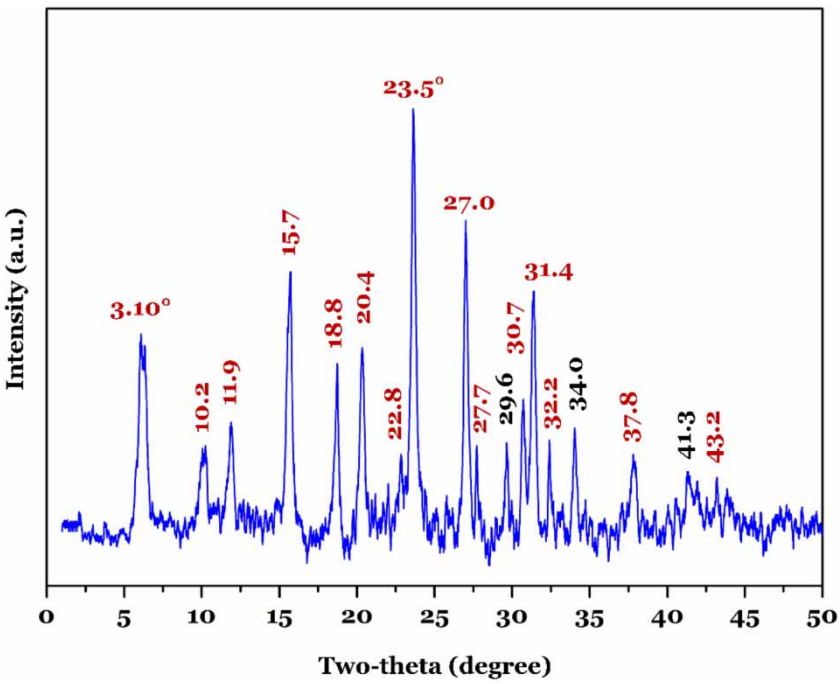

Figure 4 | XRD spectrum of the composites AlSi/NaY (20/80).

Effect of the ratios of AlSi to NaY on the adsorption capacity of the resultant composites

Figure 5 shows the adsorption isotherms of Cu^{2+}, Sr^{2+}, and Pb^{2+} ions onto the mesoporous aluminosilicate (AlSi), zeolite (NaY), and their composites synthesized from different mass ratios of AlSi/NaY (50/50 and 20/80). In general, the shape of adsorption isotherm of three selected metals belongs to H-type for the zeolite and L-type for the aluminosilicate and composites (Moreno-Castilla 2004).

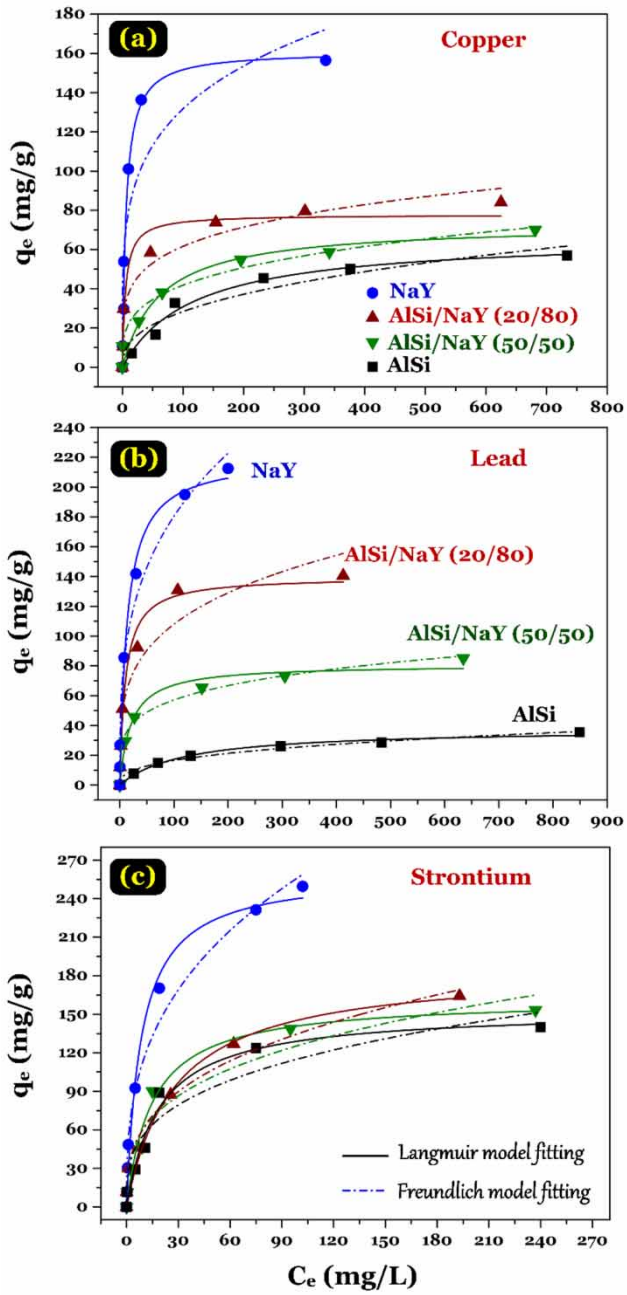

Figure 5 | Adsorption isotherm of copper, lead, and strontium by NaY, AlSi, and their composites in single aqueous solution.

The difference in the shape of the adsorption isotherm might result from differing primary adsorption mechanisms among them.

Figure 5 demonstrates that the adsorption capacity of the prepared adsorbents towards metal ions (Cu^{2+}, Pb^{2+}, and Sr^{2+}) decreased in the following order: zeolite > AlSi/NaY (20/80) > AlSi/NaY (50/50) > aluminosilicate. Aluminosilicate exhibited higher S_{BET} and V_{Total} values than zeolite. If the pore filling plays a key role in the adsorption mechanism, the adsorption capacity of aluminosilicate towards three metal ions in solution will be higher than that of zeolite. However, zeolite exhibited excellent adsorption capacities to the metal ions compared to aluminosilicate, suggesting the existence of other dominant interactions in the adsorption mechanism. The sodium element in the surface of zeolite (Figure 2(d)) has been acknowledged as exchangeable ions that have a high affinity to toxic metal ions in solution (Chao & Chen 2012; Araissi *et al.* 2015; Tran *et al.* 2018; Liang *et al.* 2020). Therefore, ion exchange between Na^{+} ions in the surface of zeolite and other metal ions (Cu^{2+}, Pb^{2+}, or Sr^{2+}) in solution is regarded as a dominant adsorption mechanism. In contrast, aluminosilicate did not exhibit the sodium element on its surface, so the ion-exchange mechanism (similar to the zeolite case) is ruled out. Aluminosilicate can adsorb metal ions (Cu^{2+}, Pb^{2+}, or Sr^{2+}) in solution through surface complexation between the oxygen-containing functional groups on its surface and metal ions in solution (Sepehrian *et al.* 2010; Tsai *et al.* 2019). As described in the section Preparation of adsorbent, during the synthesis of aluminosilicate, cetylpyridinium chloride has been used as a template, the resultant aluminosilicate might contain the nitrogen-containing functional groups derived from cetylpyridinium. The EDX technique (Figure 2) cannot distinguish between Si and N elements. Those elements often share a similarity in the energy value (overlapped energy peaks). Therefore, the surface complexation between the nitrogen atom-containing functional groups on the aluminosilicate's surface and metal ions in solution might be a less-important mechanism (Chao & Chen 2012; Özdemir & Yapar 2020). Those conclusions are supported by analysing the adsorption capacity and the properties of the resultant composites. The AlSi/NaY (50/50) and AlSi/NaY (20/80) materials shared a similarity in their textural properties (Table 1) such as S_{BET} and V_{Total} (380 m^2/g and 0.277 cm^3/g for the former; 370 and 0.254 cm^3/g for the latter). However, AlSi/NaY (20/80) exhibited a higher adsorption capacity to the selected metals in water media than AlSi/NaY (50/50) (Figure 5). The result confirmed again the negligible role of pore filling in the adsorption process of the metal ions. A higher amount of zeolite used led to a higher adsorption capacity of the resultant composites: AlSi/NaY (20/80) > AlSi/NaY (50/50), suggesting the important contribution of the ion exchange in the adsorption mechanism rather than the surface complexation.

Adsorption isotherm modeling

For modelling of the selected model isotherms, various statistic parameters (R^2 and χ^2) were calculated, and the results (Table 2) indicated that the Langmuir model was more suitable for describing the adsorption process of each metal ion (Cu^{2+}, Sr^{2+}, or Pb^{2+}) onto the selected adsorbents. Figure 6 shows that the maximum adsorption capacity of the synthesized adsorbents followed the decreasing order of $Sr^{2+} > Cu^{2+} > Pb^{2+}$, suggesting that they have a higher affinity to radioactive Sr^{2+} ions than potentially toxic metals (Cu^{2+} and Pb^{2+} ions) under the non-competitive adsorption.

Furthermore, to explore the adsorption mechanism, the amounts of metal ions adsorbed and Na^+ ions exchanged (or desorbed) during the adsorption process were compared (Table 3). For the zeolite (NaY) sample, the ratios of $q_{e,exchange}/q_{e,adsorption}$ in the case of binary (Cu^{2+} and Sr^{2+}) and multiple (Cu^{2+}, Pb^{2+}, and Sr^{2+}) solutions were 0.94 and 0.97, respectively. Those ratios are close to 1.0, suggesting that the ion exchange mechanism was dominant for the adsorption of target metals onto the zeolite (Tran *et al.* 2019). Similarly, some previous studies demonstrated that ion exchange played a dominant role in the adsorption mechanism between potentially toxic metals (Cu^{2+}, Ni^{2+}, and Pb^{2+}) and Na-zeolite (Tran *et al.* 2018), potentially toxic metals (Cu^{2+}, Ni^{2+}, Zn^{2+}, Ni^{2+}, and Pb^{2+}) and NaY zeolite (Chao & Chen 2012), Sr^{2+} and aluminosilicate zeolite (Liang *et al.* 2020), and Sr^{2+} and zeolite 4A (Araissi *et al.* 2015). Notably, the amount of Na^+ desorbed during metal ions adsorption on the aluminosilicate (AlSi) sample was not detected (data not shown). Such a conclusion is consistent with the EDX data (Figure 2(e)) – the absence of Na in the surface of aluminosilicate. Therefore, the ion-exchange mechanism (with Na^+ ions) might not exist in the adsorption process of target metal ions onto the aluminosilicate.

To sum up, the dominant mechanism for the adsorption process by zeolite was ion exchange; meanwhile, that by aluminosilicate was the surface inner-sphere complexation through the oxygen-functionality on the surface. Their composites might adsorb the metal ions in solution through the ion exchange and inner-sphere complexation. Pore filling played a less important role in the adsorption process by zeolite, aluminosilicate, and their composites.

Adsorption capacity of the resultant composites in single, binary, and multiple solutions of metal ions

To determine the possibility of selective adsorption by the synthesized samples, experiments were performed with single (Cu^{2+}, Sr^{2+}, or Pb^{2+}), binary (Cu^{2+} and Sr^{2+}), and

Table 2 | Relevant parameters of the Langmuir and Freundlich adsorption isotherms of single metal onto mesoporous aluminosilicate (AlSi), zeolite (NaY), and their composites (AlSi/NaY; wt.%/wt.%)

	Langmuir model					Freundlich model		
	Q_{max} (mg/g)	K_L (L/mg)	R^2 —	χ^2 —	K_F (mg/g)/(mg/L)^n	n —	R^2 —	χ^2 —
1. For Cu^{2+} adsorption								
Zeolite	161	0.161	0.982	68.8	47.6	0.221	0.834	639
Aluminosilicate	66.5	0.009	0.983	8.50	4.70	0.390	0.929	35.5
AlSi/NaY (20/80)	77.8	0.194	0.954	51.5	23.0	0.214	0.946	63.7
AlSi/NaY (50/50)	73.0	0.016	0.961	26.5	11.6	0.278	0.981	12.8
2. For Pb^{2+} adsorption								
Zeolite	220	0.073	0.985	120	44.5	0.304	0.982	144
Aluminosilicate	37.9	0.008	0.985	2.30	3.10	0.363	0.986	2.20
AlSi/NaY (20/80)	140	0.096	0.982	59.3	33.1	0.257	0.926	240
AlSi/NaY (50/50)	80.7	0.049	0.976	24.0	20.3	0.225	0.990	10.0
3. For Sr^{2+} adsorption								
Zeolite	260	0.119	0.985	151	51.9	0.347	0.979	206
Aluminosilicate	153	0.054	0.977	70.5	27.6	0.311	0.914	263
AlSi/NaY (20/80)	186	0.036	0.963	141	28.3	0.340	0.978	411
AlSi/NaY (50/50)	162	0.067	0.977	86.4	29.9	0.312	0.939	228

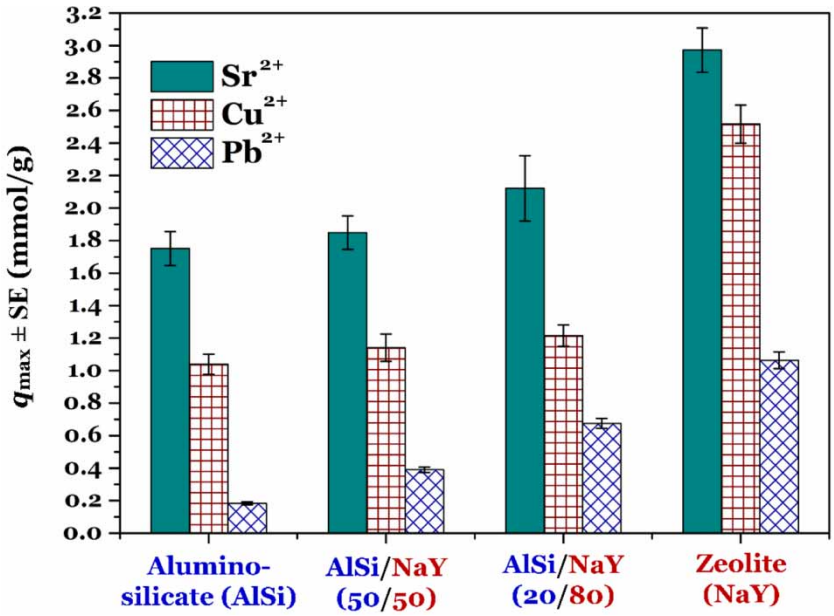

Figure 6 | Maximum adsorption capacity of adsorbent ($q_{max} \pm$ Standard Error; calculated from the Langmuir model) towards selected metal ions in single aqueous solution.

Table 3 | Comparison of amounts of metal ions adsorbed and Na^+ ions exchanged (or desorbed) during the adsorption process

	$q_{e,adsorption}$ (mmol/kg) Toxic metals	$q_{e,exchange}$ (mmol/kg) Na^+	$q_{e,exchange}/q_{e,adsorption}$
1. Binary adsorption (Cu^{2+} and Sr^{2+})			
Zeolite (NaY)	837	788	**0.94**
Aluminosilicate (AlSi)	99	–	–
AlSi/NaY (50/50)	261	108	0.41
AlSi/NaY (20/80)	307	245	0.80
2. Multiple adsorption (Cu^{2+}, Pb^{2+}, and Sr^{2+})			
Zeolite (NaY)	752	730	**0.97**
Aluminosilicate (AlSi)	576	–	–
AlSi/NaY (50/50)	569	76	0.13
AlSi/NaY (20/80)	618	300	0.49

multiple (Cu^{2+}, Sr^{2+}, and Pb^{2+}) systems (Figure 7). The results indicated that the adsorption capacities of the synthesized adsorbents remarkably decreased under binary (Cu^{2+} and Sr^{2+}) and multiple (Cu^{2+}, Sr^{2+}, and Pb^{2+}) solutions, suggesting that there was a strong competition for the available adsorption sites on the surface of the adsorbents (i.e., Na^+ ions or oxygen-containing functional groups). A similar result was reported by other scholars (Huang *et al.* 2016; Liang *et al.* 2020). The adsorption mechanism of metal ions onto the adsorbent under binary and multiple solutions is often strongly dependent on many factors (i.e., the properties of adsorbents and natures of adsorbates in solution). Therefore, it is hard to give strong evidence of what are the primary adsorption mechanisms occurring during the adsorption process. This is a limitation of this study that should be continued to tackle by some further investigations in the future.

Compassion of adsorption capacity of the resultant composites and other adsorbents

Table 4 indicates the Langmuir maximum adsorption capacity (Q_m, mg/g) of the target adsorbent materials (zeolite, aluminosilicate, and its AlSi/NaY (20/80) composite) in this study and other adsorbent solids in the literature. The commercial zeolite (NaY) exhibited an excellent adsorption capacity towards Sr^{2+} (260 mg/g), Pb^{2+} (220 mg/g), and Cu^{2+} (161 mg/g) compared to some others such as natural zeolite (93.5 mg/g for Sr^{2+} adsorption) (Abdollahi *et al.* 2020), CHA-type zeolite (11.5 mg/g for Sr^{2+}) (Liang *et al.* 2020), NaOH-treated zeolite (159 mg/g for Pb^{2+} and 60 mg/g for Cu^{2+}) (Tran *et al.* 2018), and zeolite (9.31 mg/g for Pb^{2+} and 7.86 mg/g for Cu^{2+}) (Tran *et al.* 2018).

As expected, the Langmuir maximum adsorption capacity of the newly-synthesized composite AlSi/NaY (20/80) towards radioactive Sr^{2+} ions in water (186 mg/g) was remarkably higher than that of other previously reported adsorbents; for example, rice straw-derived biochar

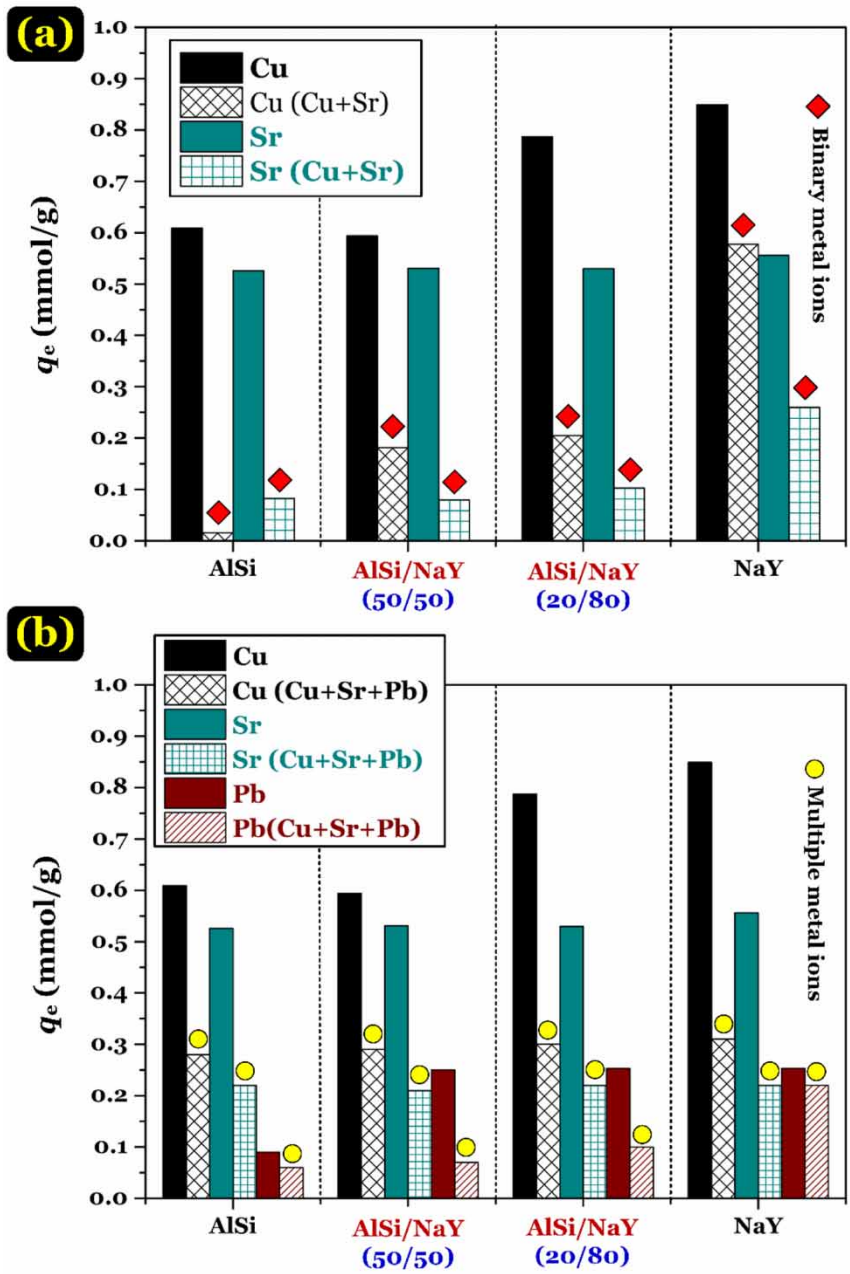

Figure 7 | Comparison of adsorption capacity of AlSi, NaY, and the AlSi/NaY composites towards selective metals under (a) single and binary adsorption and (b) single and multiple adsorption.

(176 mg/g) (Jang *et al.* 2018), natural zeolite (93.5 mg/g) (Abdollahi *et al.* 2020), CHA-type zeolite (11.5 mg/g) (Liang *et al.* 2020), and calcium-type zeolite A (Ca-zeolite A) (3.85 mg/g) and calcium phosphate/Ca-zeolite A composite (3.50 mg/g) (Watanabe *et al.* 2010), but slightly lower than that of zeolite 4A (207 mg/g) (Araissi *et al.* 2015). Furthermore, AlSi/NaY (20/80) exhibited an outstanding adsorption capacity to potently toxic metals (i.e., 140 mg/g for Pb^{2+} and 77.8 mg/g for Cu^{2+}) than some others: NaOH-treated zeolite (139 and 23.7 mg/g) (Chao & Chen 2012), hexadecyltrimethylammonium bromide-modified zeolite (135 and 24.8 mg/g)) (Chao & Chen 2012), glucose-derived spherical hydrochar (59.9 and 25.9 mg/g) (Tran *et al.* 2017a), commercial activated carbon (25.1 and 20.9 m/g) (Tran *et al.* 2017a), and zeolite (9.31 and 7.86 mg/g) (Tran *et al.* 2018). Therefore, the new composite AlSi/NaY (20/80) might serve as

Table 4 | Comparison of Langmuir maximum adsorption capacity (Q_{max}; mg/g) of the resultant composites and other adsorbents in the literature

	Q_{max} (mg/g)			
	Cu	Pb	Sr	Reference
Zeolite (NaY)	161	220	260	This study
Aluminosilicate (AlSi)	66.5	37.9	153	This study
AlSi/NaY (20/80) composite	**77.8**	**140**	**186**	**This study**
Mesoporous aluminosilicate composite	64.5	–	–	Tsai *et al.* (2019)
NaOH-treated zeolite	60.0	159	–	Tran *et al.* (2018)
NaOH-treated zeolite (Na-Y)	23.7	139	–	Chao & Chen (2012)
Hexadecyltrimethylammonium bromide-modified Na-Y zeolite	24.8	135	–	Chao & Chen (2012)
Spherical hydrochar	25.9	59.9	–	Tran *et al.* (2017a)
Commercial activated carbon	20.9	25.1	–	Tran *et al.* (2017a)
Zeolite	7.86	9.31	–	Tran *et al.* (2018)
Zeolite 4A	–	–	207	Araissi *et al.* (2015)
Rice straw-derived biochar	–	–	176	Jang *et al.* (2018)
Natural zeolite	–	–	93.5	Abdollahi *et al.* (2020)
CHA-type zeolite	–	–	11.5	Liang *et al.* (2020)
Calcium phosphate/Ca-zeolite composite	–	–	3.50	Watanabe *et al.* (2010)
Calcium-type zeolite (Ca-zeolite)	–	–	3.85	Watanabe *et al.* (2010)

promising cost-effective adsorbent for removing toxic metals from water environments.

CONCLUSIONS

New AlSi/NaY mesoporous composites (based on aluminosilicate and zeolite) were synthesized by the template co-precipitation method. The textural characteristics, surface morphology, element composition, crystal structure, and surface functional groups were studied by the nitrogen adsorption/desorption method, the SEM, EDX, XRD, and FTIR techniques. The prepared composites – AlSi/NaY (5/95), AlSi/NaY (10/90), AlSi/NaY (15/85), AlSi/NaY (20/80), and AlSi/NaY (50/50)–exhibited advantageous textural properties such as S_{BET} (370–631 m^2/g), S_{Micro} (196–550 m^2/g), and pore diameters (2.20–2.91 nm). The adsorption isotherms were well described by the Langmuir model. The maximum adsorption capacities (Q_m) of adsorbate in single-component solution (Sr^{2+}, Pb^{2+}, or Cu^{2+}) onto the adsorbents followed the decreasing order: zeolite (260, 220, or 161 mg/g) > AlSi/NaY (20/80) composite (186, 140, or 77.8 mg/g) > aluminosilicate (153, 37.9, or66.5 mg/g, respectively). The comparison of the amounts of metal ions adsorbed and Na^+ ions desorbed confirmed the dominant ion-exchange mechanism for adsorbing metal ions on the NaY zeolite. Meanwhile, the inner-sphere surface complexation played an important role in adsorbing metal ions onto aluminosilicate. The adsorption process of metal ions onto the AlSi/NaY mesoporous composites mainly involved ion-exchange and surface complexation. Pore filling had less contribution to adsorbing metal ions in solution by aluminosilicate, zeolite, and their composite. The prepared adsorbents are promising materials for treating toxic metal ions in wastewater.

DATA AVAILABILITY STATEMENT

All relevant data are included in the paper or its Supplementary Information.

REFERENCES

Abdollahi, T., Towfighi, J. & Rezaei-Vahidian, H. 2020 Sorption of cesium and strontium ions by natural zeolite and management of produced secondary waste. *Environmental Technology & Innovation* **17**, 100592.

Araissi, M., Ayed, I., Elaloui, E. & Moussaoui, Y. 2015 Removal of barium and strontium from aqueous solution using zeolite 4A. *Water Science and Technology* **73** (7), 1628–1636.

Chao, H.-P. & Chen, S.-H. 2012 Adsorption characteristics of both cationic and oxyanionic metal ions on hexadecyltrimethylammonium bromide-modified NaY zeolite. *Chemical Engineering Journal* **193–194**, 283–289.

Chowdhury, R., Ramond, A., O'Keeffe, L. M., Shahzad, S., Kunutsor, S. K., Muka, T., Gregson, J., Willeit, P., Warnakula, S., Khan, H., Chowdhury, S., Gobin, R., Franco, O. H. & Di Angelantonio, E. 2018 Environmental toxic metal contaminants and risk of cardiovascular disease: systematic review and meta-analysis. *BMJ* **362**, k3310.

Huang, F.-C., Han, Y.-L., Lee, C.-K. & Chao, H.-P. 2016 Removal of cationic and oxyanionic heavy metals from water using hexadecyltrimethylammonium-bromide-modified zeolite. *Desalination and Water Treatment* **57** (38), 17870–9.

Jamaly, S., Darwish, N. N., Ahmed, I. & Hasan, S. W. 2014 A short review on reverse osmosis pretreatment technologies. *Desalination* **354**, 30–38.

Jang, J., Miran, W., Divine, S. D., Nawaz, M., Shahzad, A., Woo, S. H. & Lee, D. S. 2018 Rice straw-based biochar beads for the removal of radioactive strontium from aqueous solution. *Science of The Total Environment* **615**, 698–707.

Kalaycı, T. & Bardakçı, B. 2014 A spectroscopic investigation for the adsorption of 4-nitrophenol onto synthetic zeolites. *Protection of Metals and Physical Chemistry of Surfaces* **50** (6), 709–714.

Li, X., Kant, A., He, Y., Thakkar, H. V., Atanga, M. A., Rezaei, F., Ludlow, D. K. & Rownaghi, A. A. 2016 Light olefins from renewable resources: selective catalytic dehydration of bioethanol to propylene over zeolite and transition metal oxide catalysts. *Catalysis Today* **276**, 62–77.

Liang, J., Li, J., Li, X., Liu, K., Wu, L. & Shan, G. 2020 The sorption behavior of CHA-type zeolite for removing radioactive strontium from aqueous solutions. *Separation and Purification Technology* **230**, 115874.

Lopes, A. C., Martins, P. & Lanceros-Mendez, S. 2014 Aluminosilicate and aluminosilicate based polymer composites: present status, applications and future trends. *Progress in Surface Science* **89** (3), 239–277.

Luo, Z., Gao, M., Yang, S. & Yang, Q. 2015a Adsorption of phenols on reduced-charge montmorillonites modified by bispyridinium dibromides: mechanism, kinetics and thermodynamics studies. *Colloids and Surfaces A: Physicochemical and Engineering Aspects* **482**, 222–230.

Luo, Z., Gao, M., Ye, Y. & Yang, S. 2015b Modification of reduced-charge montmorillonites by a series of Gemini surfactants: characterization and application in methyl orange removal. *Applied Surface Science* **324**, 807–816.

Morales-Ospino, R., Goltzman, Y., Torres, A. E. B., Vilarrasa-García, E., Bastos-Neto, M., Cavalcante, C. L., Azevedo, D. C. S., Marques, C. R. M., de Aquino, T. F. & de Oliveira, V. R. 2020 Assessment of the potential use of zeolites synthesized from power plant fly ash to capture CO_2 under post-combustion scenario. *Adsorption*. doi.org/10.1007/s10450-020-00245-0.

Moreno-Castilla, C. 2004 Adsorption of organic molecules from aqueous solutions on carbon materials. *Carbon* **42** (1), 83–94.

Nampi, P. P., Moothetty, P., Berry, F. J., Mortimer, M. & Warrier, K. G. 2010 Aluminosilicates with varying alumina–silica ratios: synthesis via a hybrid sol–gel route and structural characterisation. *Dalton Transactions* **39** (21), 5101–5107.

Özdemir, G. & Yapar, S. 2020 Preparation and characterization of copper and zinc adsorbed cetylpyridinium and N-lauroylsarcosinate intercalated montmorillonites and their antibacterial activity. *Colloids and Surfaces B: Biointerfaces* **188**, 110791.

Patil, D. S., Chavan, S. M. & Oubagaranadin, J. U. K. 2016 A review of technologies for manganese removal from wastewaters. *Journal of Environmental Chemical Engineering* **4** (1), 468–487.

Qian, T. & Li, J. 2015 Synthesis of Na-A zeolite from coal gangue with the in-situ crystallization technique. *Advanced Powder Technology* **26** (1), 98–104.

Seliem, M. K. & Komarneni, S. 2016 Equilibrium and kinetic studies for adsorption of iron from aqueous solution by synthetic Na-A zeolites: statistical modeling and optimization. *Microporous and Mesoporous Materials* **228**, 266–274.

Sepehrian, H., Ahmadi, S. J., Waqif-Husain, S., Faghihian, H. & Alighanbari, H. 2010 Adsorption studies of heavy metal ions on mesoporous aluminosilicate, novel cation exchanger. *Journal of Hazardous Materials* **176** (1), 252–256.

Tao, H.-C., Lei, T., Shi, G., Sun, X.-N., Wei, X.-Y., Zhang, L.-J. & Wu, W.-M. 2014 Removal of heavy metals from fly ash leachate using combined bioelectrochemical systems and electrolysis. *Journal of Hazardous Materials* **264**, 1–7.

Thommes, M., Kaneko, K., Neimark, A. V., Olivier, J. P., Rodriguez-Reinoso, F., Rouquerol, J. & Sing, K. S. 2015 Physisorption of gases, with special reference to the evaluation of surface area and pore size distribution (IUPAC technical report). *Pure and Applied Chemistry* **87** (9–10), 1051–1069.

Tran, H. N., Huang, F.-C., Lee, C.-K. & Chao, H.-P. 2017a Activated carbon derived from spherical hydrochar functionalized with triethylenetetramine: synthesis, characterizations, and adsorption application. *Green Processing and Synthesis* **6** (6), 565.

Tran, H. N., You, S.-J., Hosseini-Bandegharaei, A. & Chao, H.-P. 2017b Mistakes and inconsistencies regarding adsorption of contaminants from aqueous solutions: a critical review. *Water Research* **120**, 88–116.

Tran, H. N., Viet, P. V. & Chao, H.-P. 2018 Surfactant modified zeolite as amphiphilic and dual-electronic adsorbent for removal of cationic and oxyanionic metal ions and organic compounds. *Ecotoxicology and Environmental Safety* **147**, 55–63.

Tran, H. N., Nguyen, H. C., Woo, S. H., Nguyen, T. V., Vigneswaran, S., Hosseini-Bandegharaei, A., Rinklebe, J., Kumar Sarmah, A., Ivanets, A., Dotto, G. L., Bui, T. T., Juang, R.-S. & Chao, H.-P. 2019 Removal of various contaminants from water by renewable lignocellulose-derived biosorbents: a comprehensive and critical review. *Critical Reviews in Environmental Science and Technology* **49** (23), 2155–2219.

Tsai, C.-K., Doong, R.-a. & Hung, H.-Y. 2019 Sustainable valorization of mesoporous aluminosilicate composite from display panel glasses waste for adsorption of heavy metal ions. *Science of The Total Environment* **673**, 337–346.

Wang, Y., Tang, Y., Dong, A., Wang, X., Ren, N. & Gao, Z. 2002 Zeolitization of diatomite to prepare hierarchical porous zeolite materials through a vapor-phase transport process. *Journal of Materials Chemistry* **12** (6), 1812–1818.

Wang, G., Zhang, S., Hua, Y., Su, X., Ma, S., Wang, J., Tao, Q., Wang, Y. & Komarneni, S. 2017 Phenol and/or Zn2+ adsorption by single- or dual-cation organomontmorillonites. *Applied Clay Science* **140**, 1–9.

Wang, J., Tang, X., Liang, H., Bai, L., Xie, B., Xing, J., Wang, T., Zhao, J. & Li, G. 2020 Efficient recovery of divalent metals from nanofiltration concentrate based on a hybrid process coupling single-cation electrolysis (SCE) with ultrafiltration (UF). *Journal of Membrane Science* **602**, 117953.

Watanabe, Y., Miwa, Y., Ikoma, T., Yamada, H., Suetsugu, Y., Tanaka, J., Moriyoshi, Y. & Komatsu, Y. 2010 Long-term immobilization of strontium ions using zeolite A/calcium phosphate nanocomposites. *Journal of the Ceramic Society of Japan* **118** (1383), 1044–1049.

WHO 2011 *Guidelines for Drinking-Water Quality*, 4th edn, pp. 1–586. World Health Organization. Geneva, Switzerland.

Yang, X.-Y., Vantomme, A., Xiao, F.-S. & Su, B.-L. 2007 Ordered mesoporous aluminosilicates with very low Si/Al ratio and stable tetrahedral aluminum sites for catalysis. *Catalysis Today* **128** (3), 123–128.

Zayed, A. M., Selim, A. Q., Mohamed, E. A., Abdel Wahed, M. S. M., Seliem, M. K. & Sillanpää, M. 2017 Adsorption characteristics of Na-A zeolites synthesized from Egyptian kaolinite for manganese in aqueous solutions: response surface modeling and optimization. *Applied Clay Science* **140**, 17–24.

First received 22 March 2020; accepted in revised form 16 August 2020. Available online 26 August 2020